SPACE TELESCOPE SCIENCE INSTITUTE
Operated for NASA by AURA

Instrument Science Report WFC3 2005-24

WFC3 Thermal Vacuum Testing: IR Science Performance Monitor

H. Bushouse and O. Lupie
August 16, 2005

ABSTRACT

During WFC3 thermal-vacuum testing in September and October 2004, the IR19 test procedure, "IR Science Performance Monitor," was executed eight times - twice in ambient conditions and six times in thermal-vacuum. This procedure tests and monitors the stability of detector bias, darks, flats, and both unresolved and resolved sources. The results show very good repeatability of bias, dark, photometric, PSF, and flatfield measurements.

1. Introduction

The WFC3 IR camera must maintain high stability in its performance over month- and year-long time scales if it is to provide reliable scientific data. The IR19 test procedure, described in detail by Reid et al. 2004, provides monitoring of the scientific performance of the IR channel during ground testing. The basic science functions include darks, internal and external flats at multiple wavelengths, resolved sources to measure photometric throughput and unresolved sources to monitor optical quality. The data allow for the measurement of bias level, dark current, read noise, dead and hot/cold pixels, optical throughput, and PSF quality, as well as the stability and repeatability of all of these characteristics.

The IR19S01 Science Mission Specification (SMS) was executed a total of six times during the course of thermal-vacuum testing of WFC3 in September and October 2004. In addition, two iterations of SMS IR19S04 were performed under ambient conditions. The first was before chamber pump-down occurred and the second was after the chamber had been returned to ambient conditions following thermal-vacuum tests. Table 1 lists the

dates and other pertinent information for each of the runs of these SMS's. All tests were run on Rockwell IR FPA #64 installed in the WFC3 IR channel.

Table 1. Test Run Information

Run #	Date (UT)	Day of Year	SMS	Environment	FPA Temp (C)
A1	30-Aug-2004	243	IR19S04	Ambient	+23.9
1	16-Sep-2004	260	IR19S01	T/V	-123.1
2	19-Sep-2004	263	IR19S01	T/V	-123.1
3	22-Sep-2004	266	IR19S01A	T/V	-123.1
4	26-Sep-2004	270	IR19S01A	T/V	-123.1
5	29-Sep-2004	273	IR19S01B	T/V	-123.1
6	03-Oct-2004	277	IR19S01B	T/V	-123.1
A2	20-Oct-2004	294	IR19S04	Ambient	+22.9

2. Test Contents

The IR19S01 SMS consists of a total of 21 exposures. The parameters for the exposures are listed in Table 2. All exposures were obtained using a commanded detector gain setting of 2.5 e^-/DN, which results in a mean actual gain of 2.47 e^-/DN (Hilbert 2005), and a commanded detector bias offset value of 190 (~3.0 volts). There is a combination of full-frame and 64x64 pixel subarray exposures, as well as RAPID and STEP25 readout sample sequence modes. The RAPID mode reads the detector as fast as possible, resulting in sample spacings of ~4.5 seconds for full-frame images and ~0.06 seconds for 64x64 subarray images. The STEP25 readout sequence uses five fast reads at the beginning of the sequence, followed by spacings of 25 seconds between the remaining reads.

Matching darks were obtained for each of the full-frame, subarray, and sample sequence modes, which were used to calibrate the science exposures for each of those modes. A combination of point source, extended source, and flatfield exposures was also obtained. The point source exposures are used to monitor optical quality and PSF characteristics. The extended source exposures are used in conjunction with flux calibration measurements performed by the CASTLE optical stimulus (OS) in order to monitor the absolute throughput of WFC3 at different wavelengths. Flatfields were obtained at different wavelengths, using both the internal WFC3 calibration subsystem lamps and the external OS lamps.

The IR19S04 SMS includes a dark image obtained using a special detector readout timing pattern, in which only one reference pixel row in each detector quadrant is read out, which is accomplished in a short enough amount of time to avoid saturation by dark current at room temperature. The single row is read 512 times, in order to build a full-frame image. These images can be used to assess read noise in ambient conditions.

Table 2. IR19S01 Exposure Parameters

ObsID (1)	Image Type (2)	Sample Sequence (3)	NSAMP (4)	Image Size (5)	Exptime (sec) (6)	Filter (7)	Internal Lamp (8)	OS Lamp (9)	OS λ (nm) (10)	OS BW (nm) (11)	OS Img Pos (12)	Flux Cal (13)
01	Dark	Rapid	16	Sq64	0.91	-	-	-	-	-	-	-
02	Dark	Rapid	16	Full	67.05	-	-	-	-	-	-	-
04	Dark	Step25	16	Full	279.93	-	-	-	-	-	-	-
06	Dark	Step25	16	Full	279.93	-	-	-	-	-	-	-
07	Int Flat	Rapid	16	Full	67.05	F098M	QTH-3	-	-	-	-	-
09	Int Flat	Rapid	16	Full	67.05	F160W	QTH-3	-	-	-	-	-
0A	Int Flat	Rapid	16	Sq64	0.91	F160W	QTH-3	-	-	-	-	-
0B	Int Flat	Rapid	16	Full	67.05	F105W	QTH-3	-	-	-	-	-
0D	Ext Flat	Rapid	16	Sq64	0.91	F160W	-	QTH	-	-	Flat	-
0E	Ext Flat	Rapid	16	Full	67.05	F160W	-	QTH	-	-	Flat	-
0G	Ext Flat	Rapid	16	Full	67.05	F098M	-	QTH	-	-	Flat	-
0I	10μm Pt Src	Rapid	10	Full	40.23	F098M	-	QTH	980	128	-33, -11	yes
0K	10μm Pt Src	Rapid	16	Sq64	0.91	F160W	-	QTH	1600	128	-33, -11	yes
0L	10μm Pt Src	Rapid	16	Full	67.05	F160W	-	QTH	1600	128	-33, -11	yes
0N	10μm Pt Src	Rapid	16	Full	67.05	F160W	-	QTH	1600	128	IR14	yes
0P	10μm Pt Src	Rapid	16	Full	67.05	F160W	-	QTH	1600	13	-33, -11	-
0Q	200μm Src	Rapid	7	Full	26.82	F160W	-	QTH	1600	13	-33, -11	yes
0S	10μm Pt Src	Rapid	7	Full	26.82	F105W	-	QTH	1050	13	-33, -11	-
0T	200μm Src	Rapid	16	Sq64	0.91	F105W	-	QTH	1050	13	-33, -11	yes
0U	Dark	Step25	16	Full	279.93	-	-	-	-	-	-	-
0W	Dark	Step25	16	Sq64	213.80	-	-	-	-	-	-	-

Column explanations:
(1) ObsID value for the corresponding STScI ground system IPPPSSOOT-style image file name. (2) Type of image or source present. (3) Readout sample sequence name. (4) Number of samples. (5) Image size. Including reference pixels, full-frame images are 1024x1024 pixels and Sq64 images are 74x74 pixels (including reference pixels). (6) Exposure time. (7) WFC3 filter. (8) Internal cal system lamp. (9) Optical stimulus lamp. (10) OS monochromator central wavelength. (11) OS monochromator bandwidth. (12) OS image source position. (13) OS flux cal measurement obtained.

3. Data Reduction

Dark images in full-frame and SQ64 subarray modes were obtained as part of the IR19S01 science monitor program, which can, in principle, be used to construct dark calibration reference files to be used to reduce the remaining exposures in the program. However, because there were only six iterations of the science monitor performed, and the fact that only one RAPID readout dark for each of the full-frame and SQ64 subarray modes is included in each iteration of the test, it was decided to use darks obtained from the IR01 test program to construct dark reference files for the RAPID readout sequence.

A total of twenty-five RAPID full-frame and thirty SQ64 subarray darks from the IR01 program were used to construct RAPID full-frame and SQ64 subarray dark reference files. Dark references files for the STEP25 readout sequence were constructed using the STEP25 darks included in the IR19S01 science monitor program.

Before constructing the dark reference files, the raw dark images were processed with calwf3, applying reference pixel bias correction (“blevcorr”) and zero-read image subtraction (“zoffcorr”) to each raw readout. The processed exposures were then averaged, readout-by-readout, using the IRAF “imcombine” task, to construct the reference darks.

All of the remaining exposures from the six runs of IR19S01 were then processed with calwf3, using the appropriate reference files to perform dark subtraction, as needed. Calibration steps that were applied were reference pixel bias correction (“blevcorr”), zero-read subtraction (“zoffcorr”), and dark subtraction (“darkcorr”).

The warm dark images obtained from SMS IR19S04 require special processing before they can be analyzed. The algorithm that is used simply subtracts each row of the raw image from its preceding row, forming a running difference for each pair of image rows.

4. Results

4.1. Warm Dark Images

The warm dark images obtained from the IR19S04 SMS on day 243 used an incorrect setting of the detector bias offset voltage, resulting in raw pixel values that were outside the range of the A/D converters. The warm dark image obtained on day 294 was successful. Statistics of individual image rows indicate that the read noise is ~10.5 e^-/pix, which is consistent with the results from other successful runs of this procedure in early ambient tests, and also with measurements of the read noise in the reference pixels in images obtained in thermal-vaccum conditions. Therefore this read out mode is a viable means for assessing the state of the IR detector in an ambient environment.

4.2. Dark Images

Several different types of dark images are included in the IR19S01 SMS: three iterations of a STEP25 full-frame dark, one STEP25 Sq64 subarray dark, one RAPID full-frame dark, and one RAPID Sq64 subarray dark. Calwf3 processing for these images included linear fits to the signal ramp in each pixel, resulting in a final image in units of Data Numbers (DN) per second at each pixel. The mean dark current in the final images was computed by producing a histogram of all active pixel values and then fitting the histogram with a gaussian to find the location of the peak. This fitting excluded the long tail of values resulting from pixels with unusually high dark current values (see Hilbert and Robberto 2005). The resulting mean dark current values were then converted from units of DN/sec to e^-/sec using IR FPA gain values from Hilbert (2005).

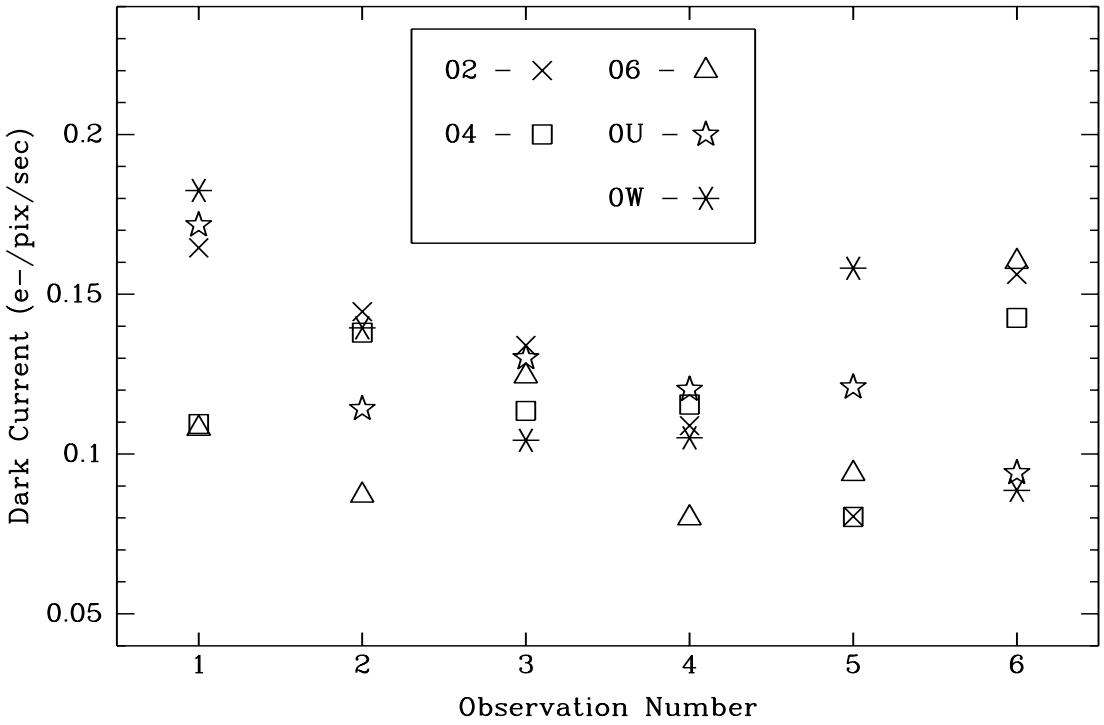

Figure 1: Dark current measurements from ObsID 02, 04, 06, 0U, and 0W images. The uncertainty on each measurement is <0.01 e^-/pix/sec, hence the variations are real.

The results for the ObsID 02, 04, 06, 0U, and 0W dark images are shown in Figure 1. The overall mean dark current from all images is 0.12 e^-/pix/sec. The values for individual images range from 0.08 to 0.18 e^-/pix/sec. The range and mean value is in very good agreement with results from the IR01 dark current procedures that were also run during thermal-vac testing (Hilbert and Robberto 2005). The uncertainty in the measured dark current value for individual images is quite small - on the order of ~0.005 e^-/pix/sec or less. This is much smaller than the size of the variations from image to image, which sug-

gests that the variations are real. Variations of this magnitude have also been seen in the analysis of the IR01 dark data that were obtained at different times during thermal-vac testing. The source of this variation is not well understood at this time, but may be associated with short- and long-term variations in FPA and cold enclosure temperatures (see Hilbert and Robberto 2005 for more details).

4.3. Flatfield Images

The IR19S01 procedure includes four flats taken using the WFC3 internal calibration subsystem and three using the external Optical Stimulus (OS). The flats are taken using a mixture of the F098M, F105W, and F160W filters and also a mixture full-frame and SQ64 subarray readout modes (see Table 2).

The same analysis procedure was followed for each set of flats. After processing with calwf3, to perform reference pixel bias level correction, zero-read subtraction, and dark subtraction, a mean flat was created by combining the six processed images, using the IRAF “imcombine” task, and then each of the individual flats was divided by the mean flat. Statistics for the mean flat and the individually flatfielded frames were measured and are presented in the following sections. Many of the individual flats were also ratioed to one another, in order to assess the stability and repeatability of the flatfield structure over time.

4.3.1. Internal Flats

Four flatfield images were taken using the WFC3 internal calibration subsystem: a full-frame F098M flat (ObsID 07), a full-frame F160W flat (ObsID 09), a SQ64 subarray F160W flat (ObsID 0A), and a full-frame F105W flat (ObsID 0B). The signal in the ObsID 09 and 0B images reached saturation levels midway through the 16-readout sample sequence. The last unsaturated readout for each image was used to construct the mean flats for these image sets. The ObsID 07 and 0A images do not reach saturation, so the final readouts were used for these.

The mean full-frame F160W flat from ObsID 09 is shown in Figure 2. All of the IR internal flats suffer from the effects of undersized optics in the IR chain of the internal calibration subsystem, which results in the flatfield images not filling the entire field of view of the detector (see Baggett 2005 for more infomation on the performance of the cal-system). Within the area of the images that is properly illuminated, the signal levels range from ~15,000 DN/pix for ObsID 07 (F098M) to ~28,000 DN/pix for ObsID’s 09 (F160W) and 0B (F105W), which corresponds to ~37,000 e^-/pix and ~72,000 e^-/pix, respectively. The rms scatter in values for an individual pixel within the stacks of six images used to construct each mean flat is ~100 DN (~250 e^-) for ObsID 07 and ~150 DN (~370 e^-) for ObsID’s 09 and 0B, which is comparable to what would be expected from pure Poisson

noise in the signal. The mean flats have uncertainties per pixel on the order of 0.5% or less.

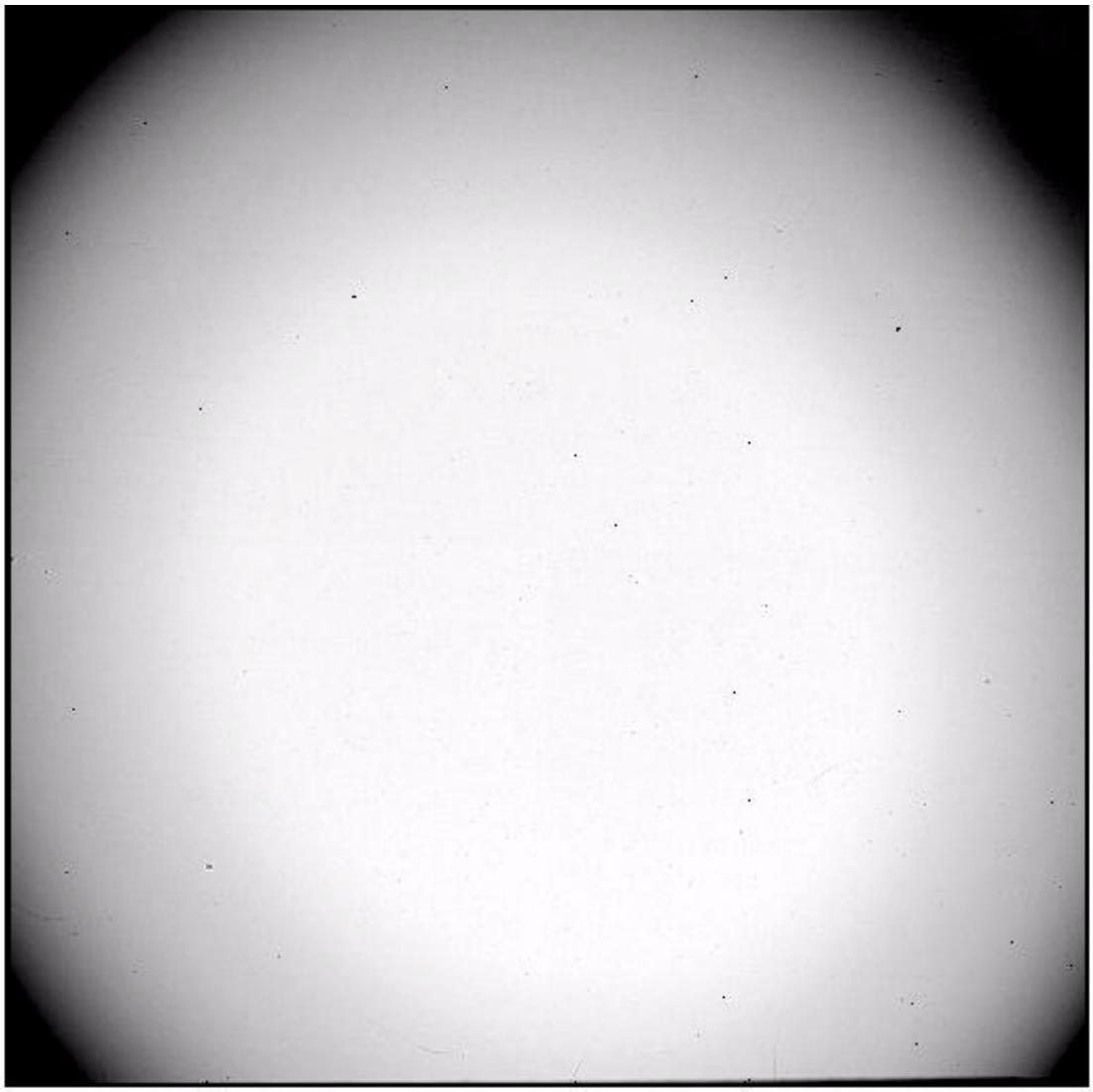

Figure 2: Internal F160W flatfield image from ObsID 09. The field is underfilled due to incorrect sizing of optical elements in the IR chain of the internal calibration system.

The ObsID 0A images, taken in the SQ64 subarray readout mode, have a much shorter total integration time (0.9 sec versus 67 secs for full-frame) and therefore also have much lower signal levels in the images of ~1450 DN/pix (~3580 e^-/pix). The rms scatter per pixel in the stack of six images used to construct the mean flat is 26 DN (64 e^-). The pixel-to-pixel scatter in the individual flats after division by the mean flat is ~1.6%, which is exactly consistent with expectations based on the measured noise in the individual images.

4.3.2. External Flats

Three external flatfield images were taken during each iteration of the science monitor, using the OS system for illumination: a SQ64 subarray F160W flat (ObsID 0D), a full-frame F160W flat (ObsID 0E), and a full-frame F098M flat (ObsID 0G). None of these exposures reached saturation level and therefore the final readouts were used to construct the mean flat for each set. However, due to an error in the OS setup, all of the external flat-field images taken on days 266 and 270 (science monitor iterations 3 and 4) have only about half the signal level of the other images. Thus when constructing the mean flats, only the four images from days 260, 263, 273, and 277 were used. The resulting mean full-frame F160W flat (ObsID 0E) is shown in Figure 3.

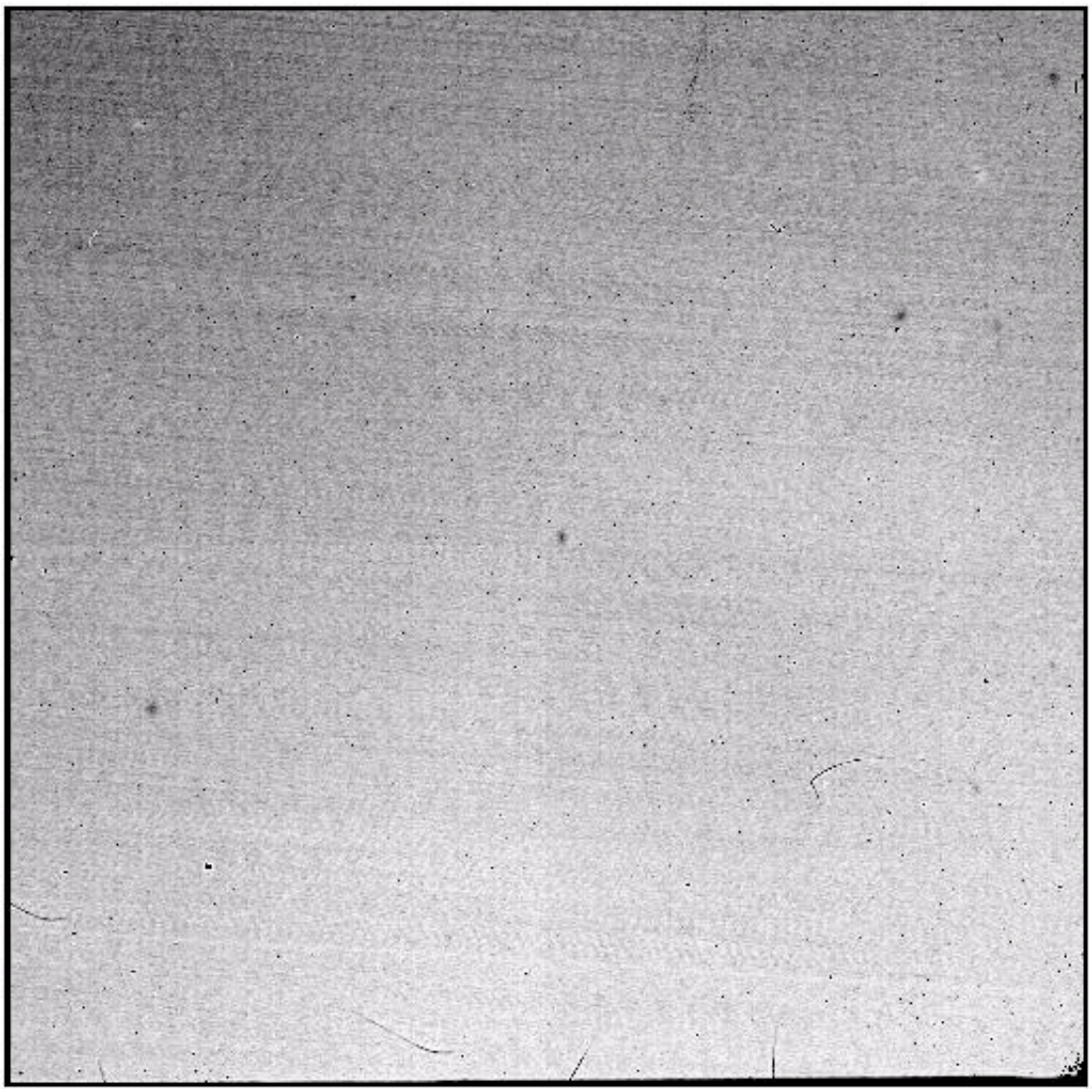

Figure 3: External F160W flatfield image from ObsID 0E. The prominent dark spots are due to dust particles on the WFC3 channel select mechanism (CSM).

The SQ64 subarray F160W flat (ObsID 0D) reached signal levels of ~6300 DN/pixel (~15,600 e^-/pix) and the rms scatter per pixel in the stack of four combined images is 65 DN (160 e^-). The rms pixel-to-pixel scatter in the individual flats after division by the mean flat is ~0.7%, which is consistent with the 160 e^- level of noise from image to image.

The full-frame external flats have mean signal levels of ~26000 e^-/pix and ~18000 e^-/pix for the F160W (ObsID 0E) and F098M (ObsID 0G) images, respectively. The rms scatter per pixel in the stacks of combined images is ~160 e^- and ~140 e^-, respectively, and the pixel-to-pixel noise in the individual flats after division by the mean flat is ~0.6% rms for both sets.

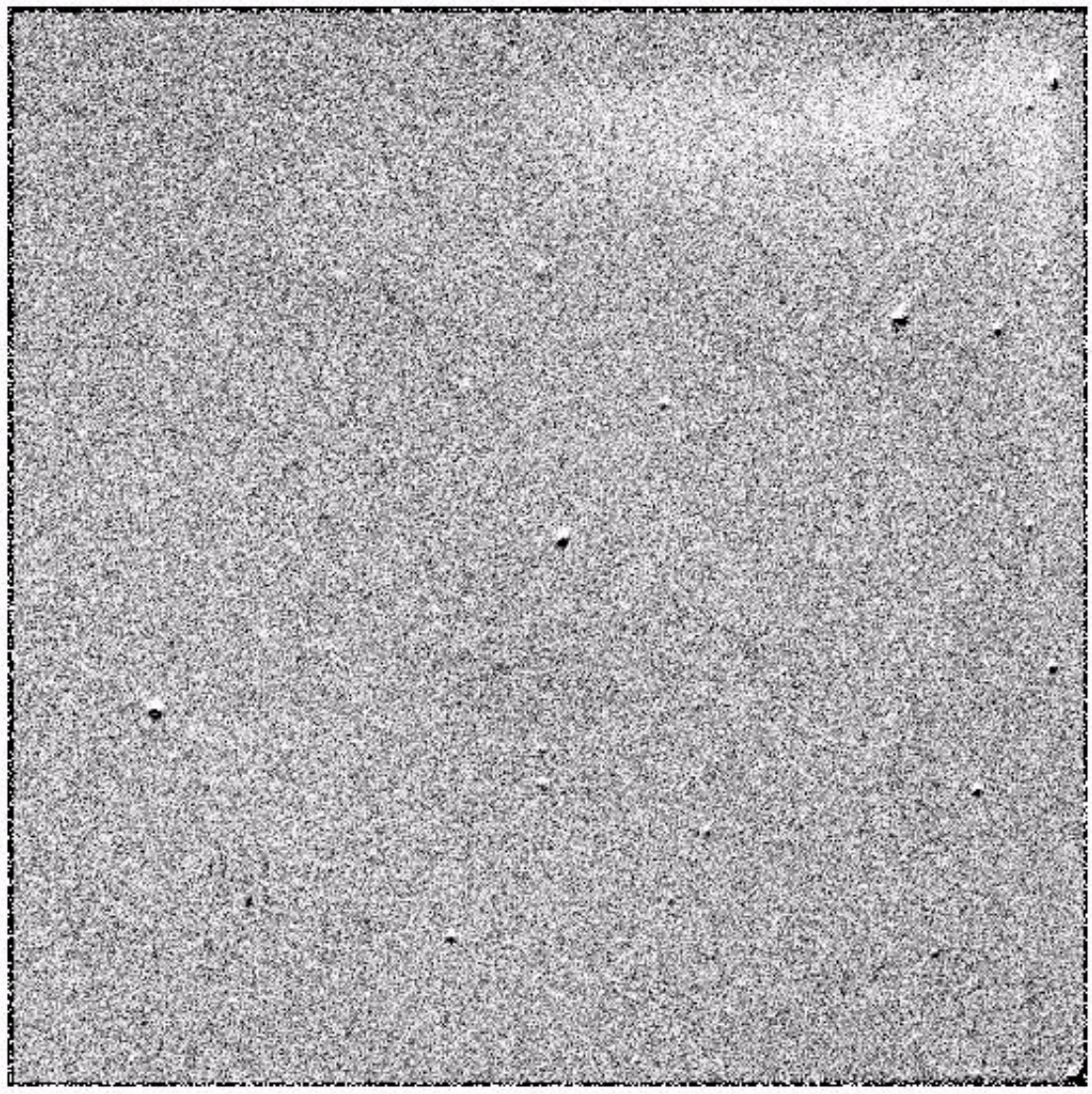

Figure 4: The ratio of two F160W flatfield images taken on days 266 and 270, showing the systematic movement of dust particles on the CSM. The particles appear as patches of adjacent light and dark spots.

The ratios of individual flats do not show any significant large-scale structure and have pixel-to-pixel noise at a level of ~1.0% rms. The only significant features that are present in the ratioed images are due to the slight movement of dust particles on the Channel Select Mechanism (CSM), which is moved into the WFC3 optical path for taking images in the IR channel. Ratios of images taken within a given science calibration episode do not indicate any significant movement of the dust features. Systematic movement of the particle pattern did occur, however, between runs 3 and 4 of the IR science monitor (days 266 and 270). During the intervening time, WFC3 was subjected to thermal cycling and a cold soak. The ratio of F160W flats taken on days 266 and 270 is shown in Figure 4. The dust particles produce features at a level of plus and minus 10% relative to the surrounding region.

4.4. PSF Monitoring Images

Point-source images were obtained near the center of the IR field of view at two different wavelengths, using the 10μm OS source fiber and a narrow-band (13 nm) monochromator setting. ObsID 0P images used a source wavelength of 1600 nm and the F160W filter, while ObsID 0S images used a 1050 nm source and the F105W filter. Encircled energy measurements were made for these images with the same analysis routine used for the regular WFC3 focus and alignment procedures (see, e.g., Hartig 2005). For the ObsID 0S images, at 1050 nm, measurements were made within apertures of 0.25” and 0.37” diameter. For the ObsID 0P images, at 1600 nm, 0.25” and 0.60” diameter apertures were used. The results are shown in Figure 5.

The mean encircled energies at 1050 nm are 0.52 (σ=0.02) and 0.74 (σ=0.03) for the 0.25” and 0.37” apertures, respectively. At 1600 nm the mean EE values are 0.41 (σ=0.014) and 0.78 (σ=0.017) for the 0.25” and 0.60” apertures, respectively. The mean values are within the range of measurements obtained from the IR08 PSF evaluation procedure data, also obtained during thermal-vac testing and show relatively little scatter throughout the 17-day time span of the IR science monitor runs. At 1600 nm the scatter is 1-2%, while at 1050 nm it is a bit higher, in the 2.5-3% range.

4.5. Photometric Monitoring Measurements

There are six exposures in the IR19S01 procedure that can be used to monitor the photometric performance and stability of the WFC3 IR channel. Four of these use the OS 10μm source fiber, which results in a point source, and two use the 200μm source fiber, which results in an extended source of ~20 pixels in diameter in IR images. The exposures were also obtained using a combination of full-frame and SQ64 subarray readout modes. OS flux calibration measurements were obtained for all of the exposures, which provides a measurement of the photon flux incident on the WFC3 pick-off mirror (POM).

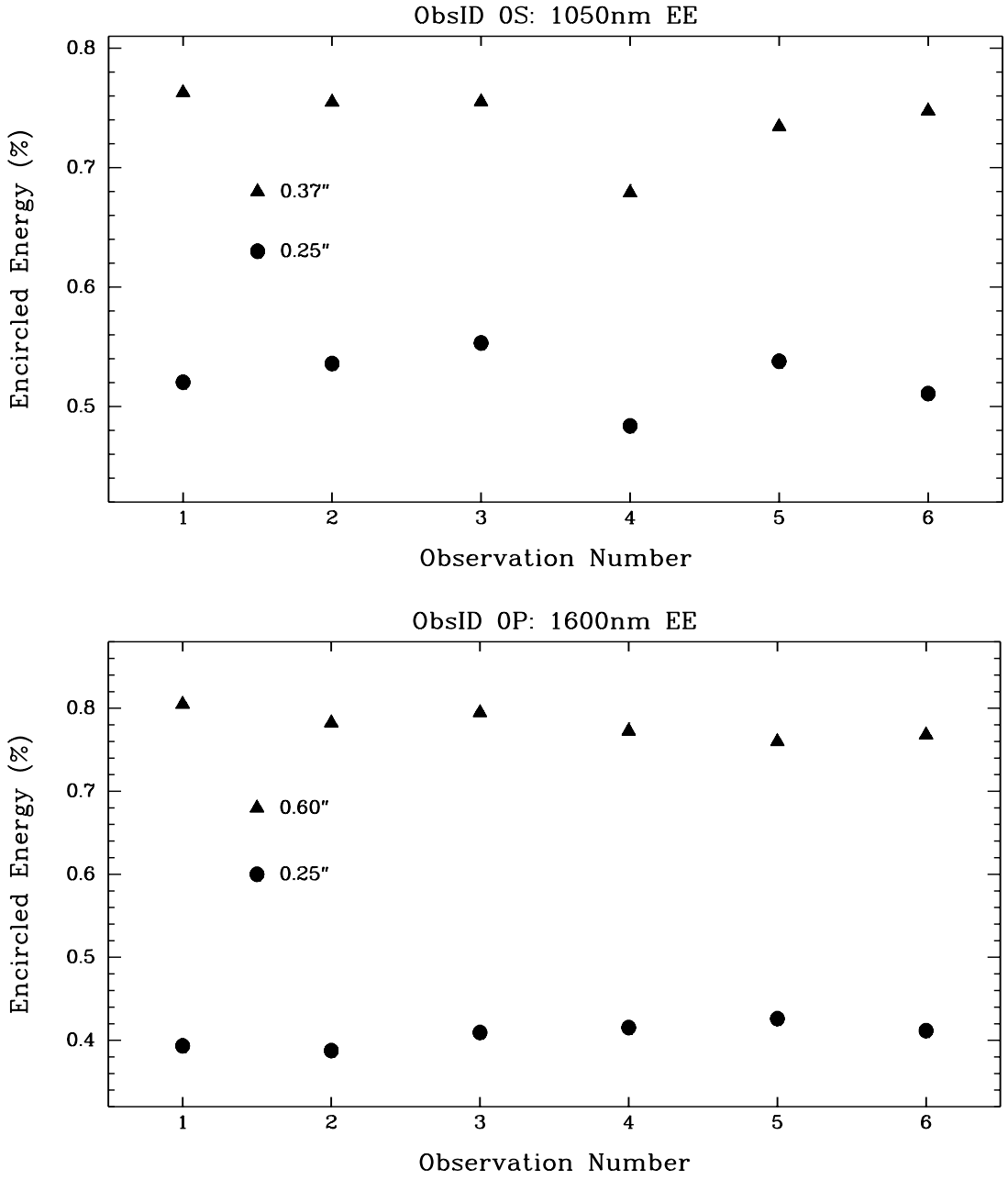

Figure 5: Encircled energy measurements from ObsID 0P and 0S images.

Aperture photometry was performed on the processed images using the IRAF “phot” routine. For the point sources in full-frame images (ObsID’s 0I, 0L, and 0N) an aperture radius of 20 pixels was used, along with a background annulus of 30 pixels radius and 5 pixels width. For ObsID 0K, which has a point source in a SQ64 subarray, an object aperture of 12 pixels radius was used and background measurements were taken using a separate aperture in another part of the image. For ObsID 0Q, which has an extended

source in a full-frame image, an object aperture of 30 pixels radius was used along with a background annulus 40 pixels in radius and 10 pixels width. For ObsID 0T, which has an extended source in one corner of a SQ64 subarray image, it was necessary to use a smaller object aperture of 12 pixels radius, due to the proximity of the source to the edge of the image. A separate background aperture was used in another part of the image.

The measured counts were normalized by the OS flux calibration measurement for each exposure, in order to track and remove variations in the OS source flux. Due to an error in the OS operations during the first run of the IR science monitor (day 260), no useable flux calibration measurements were obtained and hence the photometric measurements from the images obtained that day are not used in the following analysis. Furthermore, some additional individual exposures suffered from other types of OS errors and are also excluded. These are noted in the following sections.

4.5.1. ObsID 0I: F098M Point Source

These exposures used a point source very near the center of the IR detector. The five sets of exposures obtained in science monitor runs 2-6 were all successful and the photometry results are shown in Figure 6. The plot shows the ratio of detected to incident flux, normalized by the mean ratio of the five successful observations. The rms scatter about the mean for these five observations is 0.9%, which indicates excellent photometric stability and repeatability.

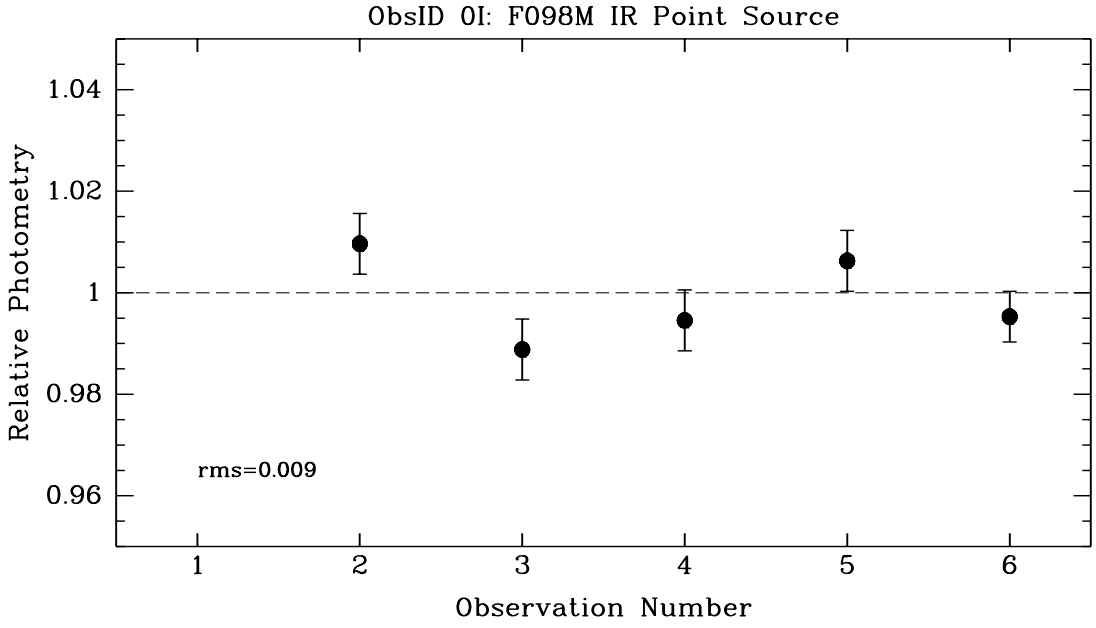

Figure 6: Photometry results for ObsID 0I images. The data have been normalized to the mean of the five successful runs (observation numbers 2-6).

4.5.2. ObsIDs 0K, 0L and 0N: F160W Point Sources

These exposures all use a broadband (130 nm) point source with a central wavelength of 1600 nm observed with the F160W filter. ObsID OK and 0L exposures place the source near the center of the field of view, while 0N has the source at the IR14 field position, which is near a corner. Additionally, ObsID 0K exposures used the SQ64 subarray readout mode, while 0L and 0N are full-frame.

The results of the photometry measurements for these exposures are shown in Figure 7. The photometry for observation number 4 (day 270) in the ObsID 0K series came out anomalously high (~8%) relative to the rest of the series and is not included in the plot in Figure 7. The cause of this anomaly is not known. The remaining four data points have an rms scatter of 1.2% about their mean.

The exposures for the fifth run of the science monitor (day 273) for ObsID's 0L and 0N suffered from an OS misconfiguration that caused the images to be irrecoverably saturated and therefore not useable. The results for the four remaining measurements are in Figure 7. The scatter about the mean is somewhat larger for these series, having rms residuals of 1.7% and 3.2%, respectively. The majority of the increased scatter is due to the results from observation number four in both sets of exposures. Analysis of the OS flux calibration measurements for these exposures suggests that the source lamp flux was drifting somewhat during the time of these exposures. Because the OS calibration measurements are obtained before each WFC3 exposure, as opposed to simultaneously with them, drift in the lamp output could be the cause of these discrepant results. Without the data for observation number four in each set, the residuals are in the 0.5-1.0% range.

4.5.3. ObsIDs 0Q and 0T: F160W and F105W Extended Sources

These exposures use a narrowband (13 nm), extended source located near the center of the field. Unfortunately, the location of the source straddles one of the CSM dust particle features mentioned in Section 4.3.2. Because the location of the particles changed during the course of testing, it was necessary to apply individual daily flatfields to these exposures in order to properly correct for the effect of the dust. The photometry results are shown in Figure 8. The rms residuals about the mean are 2.1% and 1.4%, respectively. This amount of scatter is larger than what is expected from statistical uncertainties in the aperture photometry measurements alone.

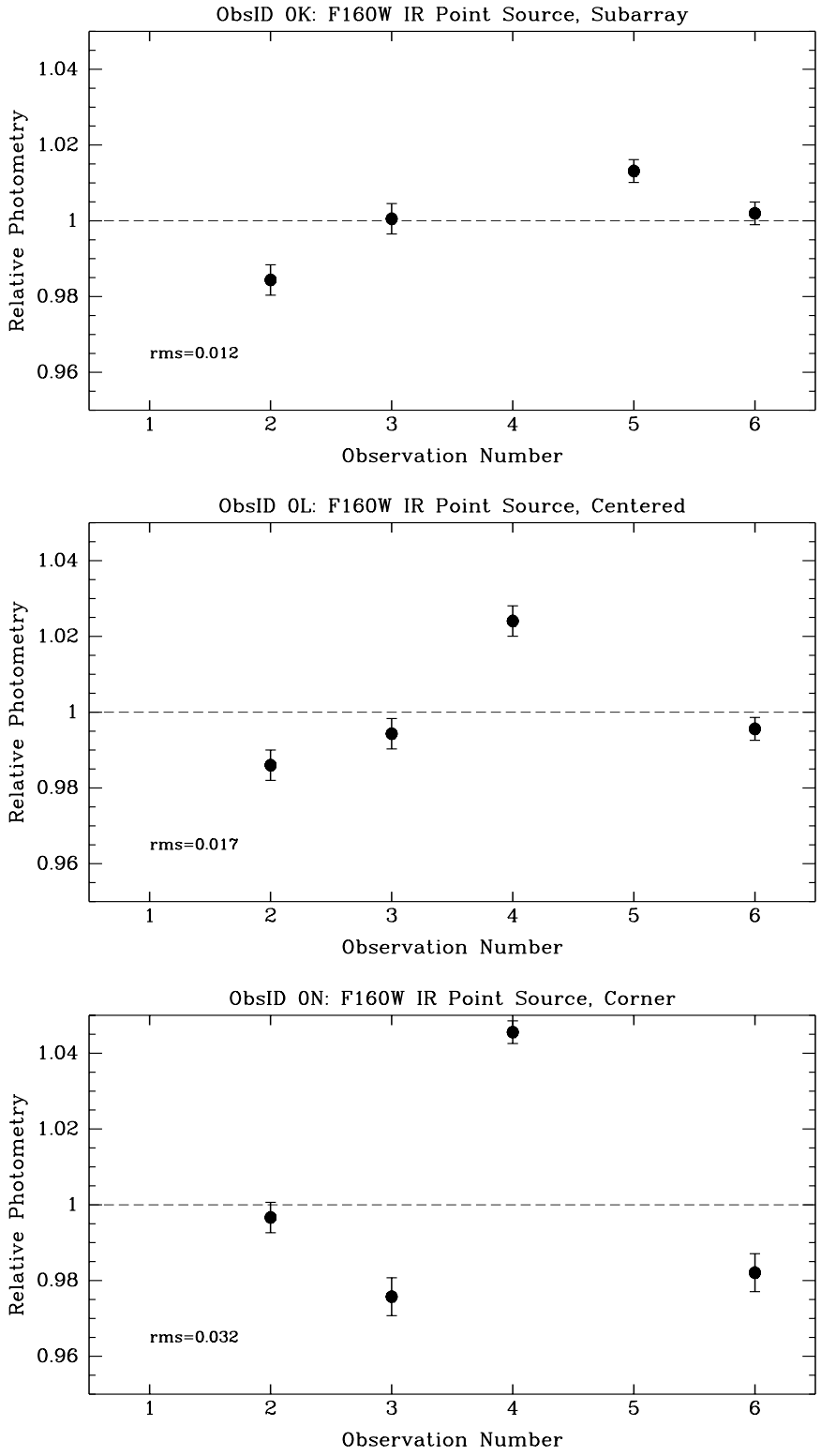

Figure 7: Photometry results for ObsID 0K, 0L, and 0N images. In all cases the data have been normalized to the mean of the four data points shown.

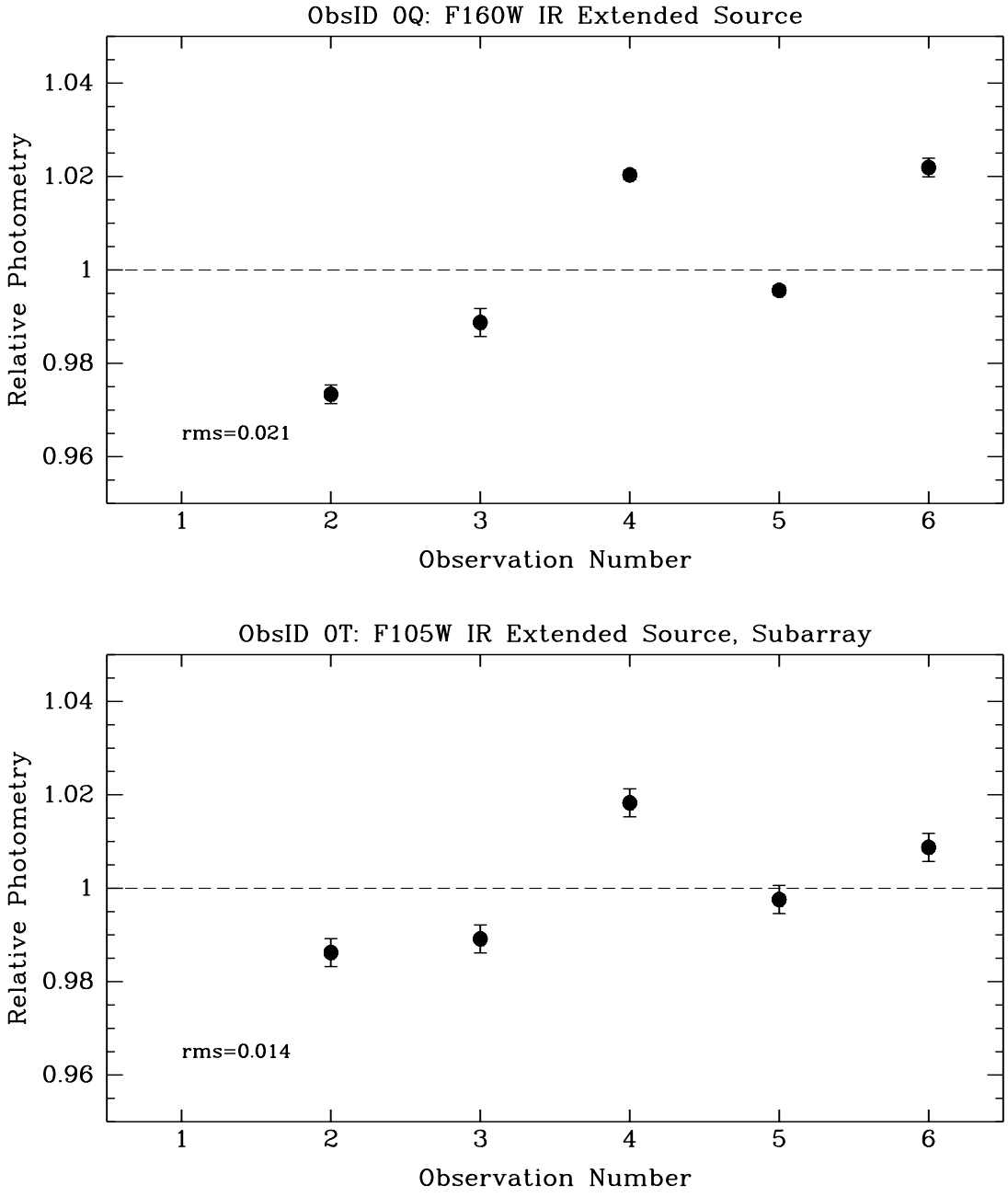

Figure 8: Photometry results for ObsID 0Q and 0T images. The data have been normalized to the mean of the five data points shown.

5. Summary

The six repetitions of the IR19S01 SMS that were executed on WFC3 during the thermal-vacuum testing performed in September-October 2004 show that the IR channel performs well and is quite stable. This holds true in spite of the fact that on several occasions throughout the course of testing the instrument safed and was restarted, the detector packages temporarily lost vacuum, and the detectors were warmed and recooled.

The mean dark current level during these tests was 0.12 e^-/pix/sec, which is well below the CEI specification of 0.4 e^-/pix/sec, but there is variability from image to image of up to ~0.05 e^-/pix/sec. Flatfielding accuracy and stability is in the 0.5-1.0% range. Encircled energy is repeatable to 1-3% and the photometric stability of this data set is in the 1-2% range.

The only instrument-related issue brought to light by these tests is the complicating effect of dust particles on the CSM on photometric measurements.

6. References

Baggett, S. 2005. “WFC3 Thermal-Vacuum and Ambient Testing: Calibration Subsystem Performance,” STScI ISR WFC3 2005-09, http://www.stsci.edu/hst/wfc3/documents/ISRs/WFC3-2005-09.pdf.

Hartig, G. 2005. “WFC3 UVIS PSF Evaluation in Thermal-Vaccum Test #1,” STScI ISR WFC3 2005-10, http://www.stsci.edu/hst/wfc3/documents/ISRs/WFC3-2005-10.pdf.

Hilbert, B. 2005. “Results of WFC3 Thermal Vacuum Testing: IR Channel Gain,” STScI ISR WFC3 2005-14, http://www.stsci.edu/hst/wfc3/documents/ISRs/WFC3-2005-14.pdf.

Hilbert, B. & Robberto, M. 2005. “WFC3-IR Thermal Vacuum Testing: IR Channel Dark Current,” STScI ISR WFC3 2005-25, http://www.stsci.edu/hst/wfc3/documents/ISRs/WFC3-2005-25.pdf.

Reid, I. N., et al. 2004. “WFC3 Science Calibration Plan Part 4: Test Procedures,” STScI ISR WFC3 2004-03, http://www.stsci.edu/hst/wfc3/documents/ISRs/WFC3-2004-03.pdf.